Field-enhanced ion transport in solids: Reexamination with molecular dynamics simulations

A. R. Genreith-Schriever and R. A. De Souza*

Institute of Physical Chemistry, RWTH Aachen University and JARA-FIT, 52056 Aachen, Germany

(Received 7 July 2016; revised manuscript received 14 November 2016; published 16 December 2016)

Classical molecular-dynamics simulations were used to examine the effect of an electric field on the mobility of oxygen ions in the model crystalline oxide CeO_2. Simulation cells containing oxygen vacancies were subjected at temperatures $1000 \leqslant T/\mathrm{K} \leqslant 1600$ to electric field strengths $0.1 \leqslant E/\mathrm{MVcm^{-1}} \leqslant 40$ to obtain the oxygen-ion mobility $u_\mathrm{i}(E,T)$. In addition, static nudged-elastic-band calculations were performed to obtain directly the forward/reverse barriers for oxygen-ion migration, $\Delta H^{\mathrm{f/r}}_{\mathrm{mig}}$. Qualitatively, u_i behaves as expected: independent of E at low values of E and exponentially dependent on E at high values. The quantitative (standard) Mott-Gurney treatment, however, underestimates $\Delta H^{\mathrm{f}}_{\mathrm{mig}}$ at high E and thus overestimates u_i. A new, superior analytical expression for $u_\mathrm{i}(E,T)$ is consequently derived.

DOI: 10.1103/PhysRevB.94.224304

The advent of memristive oxide devices is reawakening interest in the phenomenon of field-accelerated ion transport in solids. Initial interest in the phenomenon can be traced back many decades to studies of the oxidation of metals [1–4]. The recent interest has arisen not only because memristive behavior in oxides involves ion transport [5–10], but also, and more importantly, because optimal memristive devices should exhibit ultra-nonlinear switching kinetics. Memristive devices should namely switch within tens of nanoseconds between low- and high-resistance states upon application of only a few volts (the write step), but they should remain stable for up to ten years in either the low- or the high-resistance state upon repeated interrogation with voltages of a fraction of a volt (the read step). Optimal performance requires, therefore, an increase in the kinetics by a factor of 10^{16} upon an increase in voltage by a factor of only 10, an issue known as the voltage-time dilemma [6,11]. Field-enhanced ion mobility constitutes one such source of nonlinearity [11–15].

Interest in this phenomenon is also being generated, more generally, from the increasing application of oxides in nanoscale form, be it in electronic (gate dielectrics), electrochemical (Li batteries), or electrical (multilayer ceramic capacitors) devices [16,17]. Decreasing the characteristic dimension of the oxide to the nanoscale at constant operating voltage leads inevitably to huge increases in electric field strength, and thus to the possibility of field-enhanced ion transport. In some cases, this effect is unwanted, as ions that exhibit negligible mobility at low fields may become mobile, leading to losses in performance or even enhanced rates of device failure. In other cases, high fields may be beneficial, giving rise to higher ion mobilities and thus to lower internal resistances.

The standard treatment of the effect of an electric field on the rate of ion transport in a solid dates back to Verwey [1] and Mott and Gurney [2]. This treatment is based on an ion in a one-dimensional, periodic lattice executing jumps to empty neighboring sites by surmounting an activation barrier ΔH_{mig}. The applied field strength E is considered to modify the activation barrier, lowering it to $\Delta H^{\mathrm{f}}_{\mathrm{mig}}$ for forward jumps and raising it to $\Delta H^{\mathrm{r}}_{\mathrm{mig}}$ for reverse jumps, where

$$\Delta H^{\mathrm{f/r}}_{\mathrm{mig}} = \Delta H_{\mathrm{mig}} \mp |z_\mathrm{i}| e E a_\mathrm{i} \tag{1}$$

($z_\mathrm{i}e$ is the charge of the migrating ion and a_i is the distance between its initial and saddle-point configurations). In this way the probability of ion motion in the forward direction is increased and the probability of motion in the reverse direction is decreased. The net motion in the forward direction is proportional to the difference in the forward and backward rates. If the distribution of the mobile ions in the solid remains uniform, the drift velocity of the ions follows as

$$v_\mathrm{d} = 2(1-n_\mathrm{i}) a_\mathrm{i} \nu_0 \exp\left(\frac{\Delta S_{\mathrm{mig}}}{k_\mathrm{B}}\right) \times \left[\exp\left(-\frac{\Delta H^{\mathrm{f}}_{\mathrm{mig}}}{k_\mathrm{B}T}\right) - \exp\left(-\frac{\Delta H^{\mathrm{r}}_{\mathrm{mig}}}{k_\mathrm{B}T}\right)\right], \tag{2}$$

where n_i is the site fraction of ions; ν_0 is the attempt frequency; ΔS_{mig} is the activation entropy of migration; and k_B and T have their usual meanings. Combining Eqs. (1) and (2), one obtains the well-known hyperbolic sine dependence of the drift velocity on applied field,

$$v_\mathrm{d} = B \exp\left(-\frac{\Delta H_{\mathrm{mig}}}{k_\mathrm{B}T}\right) \sinh\left(\frac{|z_\mathrm{i}| e E a_\mathrm{i}}{k_\mathrm{B}T}\right), \tag{3}$$

with $B = 4(1-n_\mathrm{i}) a_\mathrm{i} \nu_0 \exp(\Delta S_{\mathrm{mig}}/k_\mathrm{B})$. For small values of E, Eq. (3) reduces to a linear law, $v_\mathrm{d} \propto E$, with the constant of proportionality being the field-independent mobility u_i. For large E, an exponential increase in v_d with increasing E is predicted, and u_i ($= v_\mathrm{d}/E$) is strongly field dependent.

Surprisingly, there is to date no direct experimental confirmation that Eq. (3)—despite its widespread use—correctly describes $u_\mathrm{i}(E)$. Part of the problem is certainly the difficulties that are encountered in investigating experimentally this effect at high fields. First, a significant increase in ion mobility is only expected, according to Eq. (3), for $E \approx (k_\mathrm{B}T)/(|z_\mathrm{i}|ea_\mathrm{i})$. For O^{2-} ions in CeO_2, for example, the field required at $T = 1250\,\mathrm{K}$ to give $u_\mathrm{i}(E)/u_\mathrm{i}(0) = 1.1$ is $E = 10^{0.5}\,\mathrm{MV\,cm^{-1}}$. Not only is this close to the fields required for dielectric breakdown, it also corresponds to applying a voltage of $V \approx 320$ V to a 1 μm thick sample. A voltage of $V_\mathrm{c} \approx 4.3$ V, however, is already sufficient at $T = 1250$ K to decompose

*desouza@pc.rwth-aachen.de

CeO_2 ($V_c = -\Delta_f G/2F$, where $\Delta_f G$ is the Gibbs formation energy of CeO_2 from the elements [18]). Second, high fields generate high current densities, which in turn lead through Joule heating to considerable increases in sample temperature. One must be able, therefore, to attribute unambiguously a measured increase in mobility to field enhancement rather than to temperature enhancement. Third, interfaces may govern the overall electrical response of the system. Pristine grain boundaries in CeO_2-based oxides, for example, exhibit lower conductivity than the bulk phase, and this is due to space-charge layers [19–25]. Observed nonlinear effects may arise, therefore, from grain boundaries (or from the electrodes) rather than from the bulk phase (although this effect may be utilized, e.g., to study grain-boundary properties [26,27]). If both electrodes are, in addition, not entirely reversible for the mobile ions, there will be a build-up of these ions at the one electrode and a depletion at the other electrode (stoichiometry polarization). Ion transport will thus take place in a sample of non-uniform composition. Fourth, electronic phenomena may come into play, e.g., the Poole-Frenkel effect, the Nordheim-Fowler effect, or the intrinsic electronic conductivity of the oxide. Again, the measured nonlinear conductivity may be due to effects other than ion motion in the bulk.

There are means of avoiding some of these issues. Murugavel and Roling [28], for instance, studied ion transport in glasses (no grain boundaries, no electronic conductivity but variable jump distances) and demonstrated that by using ac electric fields one can not only isolate the response of the bulk from that of the electrodes, but one can also unambiguously identify a field-induced enhancement in ion mobility (as opposed to one from Joule heating). Applying high ac fields is not trivial, though, and this restricted the experiments performed by Murugavel and Roling [28] to the weak nonlinear regime, i.e., the observed field enhancement was limited to $\approx$10%.

In this study we use classical molecular-dynamics (MD) simulations to examine the fundamental question of whether the Mott-Gurney expression for $u_i(E)$ [Eq. (3)] is correct. In general, both experimental and computational studies [16,28–30] assume that Eq. (3) is valid. To this end, we study the mobility of oxygen ions in a model, crystalline oxide system (oxygen-deficient CeO_2) as a function of field strength. By performing these specific simulations we avoid all of the problems facing the experimentalist and are thus able to focus exclusively on ion transport: we have neither grain boundaries nor (polarizing) electrodes in the system, neither dielectric breakdown nor decomposition, and neither electronic processes nor conductivity. Furthermore, the simulations permit excellent monitoring and control of temperature. We chose a crystalline system because, in comparison with amorphous systems, the jump distance is well defined; and we chose specifically CeO_2, not only because it is a model system for its structurally more complex but technologically more important cousin HfO_2, but also because oxygen-ion migration in CeO_2 in the low-field regime is well characterized and understood, both computationally [31–37] and experimentally [38–43].

Atomistic simulations based on the Born model of ionic solids [44] were employed. The ions are treated as classical particles that interact through long-range Coulombic interactions and through parametrized Buckingham pair-potentials (further details are given as Supplemental Material [45]). This description has been successfully applied to simulating CeO_2 in diverse cases [36,46–49]. Here the MD simulations employed $14 \times 14 \times 14$ unit cells of fluorite-structured ($Fm\bar{3}m$) ceria. Oxygen vacancies were introduced into the cell by removing oxygen ions at random. In order to compensate the charge of the vacancies, the charge of all cerium cations was decreased slightly. The site fraction of oxygen vacancies was set at $n_v = 0.10\%$, i.e., within the dilute regime. In this way, vacancies are unlikely to site block the migration of other vacancies, and the change in the charge of the cations is kept small (ca. $4 \times 10^{-3} e$). By changing the charge of all the cations rather than substituting specific Ce cations with trivalent dopant cations, we avoid introducing complexities into the transport behavior due to vacancy-dopant interactions [31–35].

Supercells of $Ce_{10976}O_{21930}$ were subjected to electric fields along the x direction (that is, along one of the three possible orthogonal jump directions), by applying an additional force $\mathbf{F} = z_i e\mathbf{E}$ to each ion. Field strengths from $10^{-3} < E/\mathrm{MV\,cm^{-1}} < 10^{1.6}$ were investigated, and the mean displacement of the oxygen ions along the x, y, and z directions was monitored. After the equilibration period, $\langle y \rangle$ and $\langle z \rangle$ were, as expected, zero, as no field was applied in these directions. $|\langle x \rangle|$, however, showed a constant, linear increase with time (see Fig. S1 [45]). The drift velocity of the oxygen ions was calculated from $v_d = d|\langle x \rangle|/dt$, from which the ion mobility can then be calculated from $u_i = v_d/E$. All simulations were performed with the LAMMPS code [50].

In Fig. 1 we plot the oxygen-ion mobility obtained from our MD simulations as a function of applied field strength. At each temperature examined, one sees, as expected, a field-independent mobility at low fields, and an exponential increase at the high fields. No data was obtained for $E > 35\ \mathrm{MV\,cm^{-1}}$, as the simulation cells exhibited, regardless of the temperature, a structural instability under the applied field: oxygen ions did not reside at well-defined sites, and after a certain amount of time, cerium ions showed similar behavior (see video [45]). For field strengths $E < 10^{-1}\ \mathrm{MV\,cm^{-1}}$ the data scattered considerably, as only a few successful ion jumps were observed during the simulations. These data are not shown in Fig. 1.

We compare in Fig. 1 the MD data with predictions of the standard Mott-Gurney treatment [Eq. (3)], taking the values for B, a_i and ΔH_{mig} given in Table S.II [45]. Although this simple expression does indicate correctly that the linear regime corresponds to $E \ll (k_B T)/(|z_i| e a_i)$, it only describes the field enhancement in the very weak-field regime (increases in u_i by a factor of 20–30%), and it clearly overestimates u_i at high field strengths, with the difference becoming larger as the temperature decreases. In fact, extrapolating our MD data to room temperature, we predict that Eq. (3) will overestimate u_i at $E = 20\ \mathrm{MV\,cm^{-1}}$ by ca. two orders of magnitude, with even larger differences at higher fields. The standard Mott-Gurney treatment is, therefore, unsatisfactory for describing highly nonlinear field enhancements, such as those required for resistively switching devices.

Also shown in Fig. 1 are the predictions of a "second-order correction" proposed by Fromhold and Cook [51]. They suggested that Eq. (1) needs to be corrected at high fields because a_i—the distance between the initial and saddle-point configurations—is shortened for forward jumps (to a_i^f) and

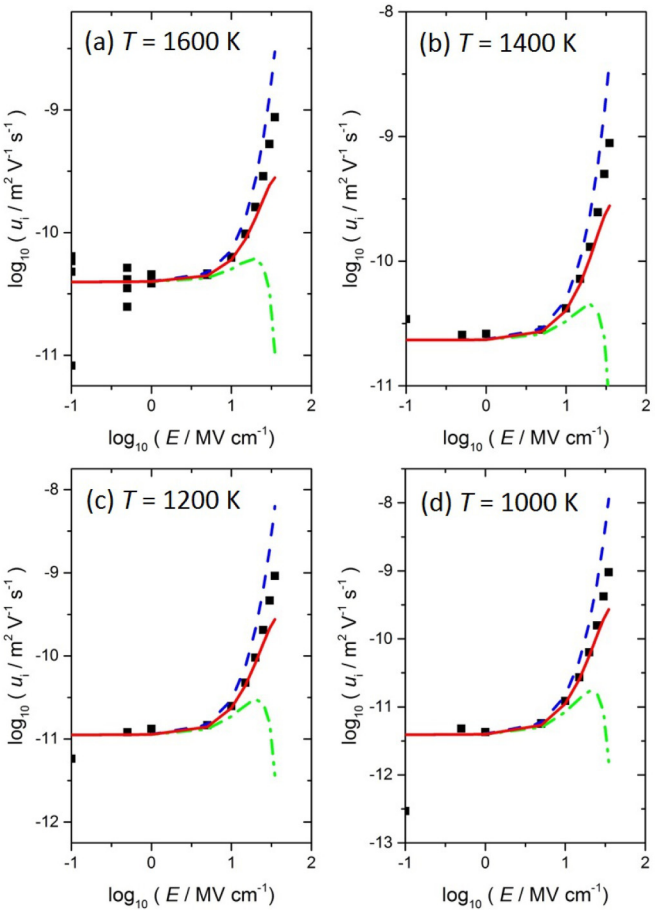

FIG. 1. Oxygen-ion mobility u_i in CeO_2 as a function of electric field E at four temperatures (a)–(d). Symbols, data from MD simulations; dashed line, Eq. (3); dashed dotted line, Eqs. (2) and (4); solid line, Eqs. (2) and (6).

lengthened for reverse jumps (to a_i^r) under the action of the field. If the energy surface for the migrating ion is cosinusoidal, Fromhold and Cook [51] showed that this shortening and lengthening leads to

$$\begin{aligned}\Delta H_{\rm mig}^{\rm f/r} &= \Delta H_{\rm mig} \mp |z_i| e E a_i^{\rm f/r} \\ &= \Delta H_{\rm mig} \mp |z_i| e E a_i \\ &\quad + \left(\frac{2|z_i| e E a_i}{\pi}\right) \arcsin\left(\frac{2|z_i| e E a_i}{\pi \Delta H_{\rm mig}}\right). \end{aligned} \tag{4}$$

Inserting Eq. (4) into Eq. (2) gives the corresponding data in Fig. 1. As one can see, this prediction, while diminishing the degree of the field enhancement, ends up severely underestimating the MD data.

If we take Eq. (4) to be correct, and disregard the ad hoc manner in which the correction was introduced, the obvious possible reason for the lack of agreement is that the energy profile of the migrating ion deviates from a cosinusoidal form. We performed, therefore, nudged-elastic-band (NEB) calculations [52] to determine the form of the energy surface. As shown in Fig. 2, the profile is in fact cosinusoidal. The activation energy obtained without applied field, $\Delta H_{\rm mig} = 0.638$ eV, is consistent with the low-field MD data, as

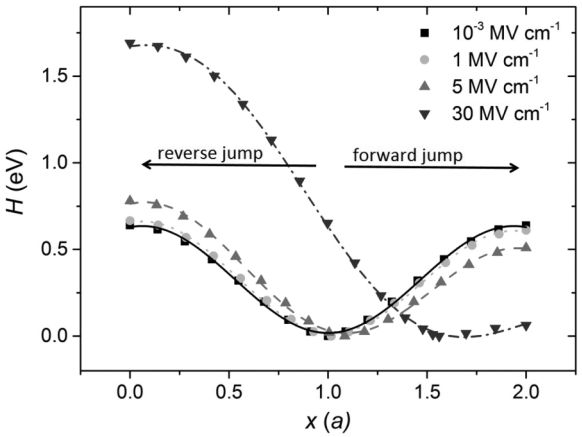

FIG. 2. Energy profiles of a migrating oxygen ion in CeO_2 executing forward and reverse jumps to neighboring vacant sites for various electric field strengths. Obtained by NEB calculations.

evident in Fig. 1. The form (cosinusoidal) and the height (ca. 0.6 eV) of the activation barrier for oxygen-ion migration in CeO_2 also agree well with literature data, including results from density-functional-theory calculations [31,32,35–37]. In addition, NEB calculations performed under applied fields (Fig. 2) indicate that a_i^f and a_i^r are indeed shortened and lengthened by the field, in the manner expected. This leaves us with a second possibility, that neither of these treatments—neither Mott and Gurney's nor Fromhold and Cook's—are quantitatively correct.

We take, therefore, a new approach. As in Ref. [51], we superimpose a linear field on a cosinusoidal energy landscape,

$$H(x) = \frac{\Delta H_{\rm mig}}{2} \cos\left(\frac{\pi x}{a_i}\right) - |z_i| e E x. \tag{5}$$

Here, however, we directly derive $\Delta H_{\rm mig}^{\rm f/r}(E)$. Specifically, by finding one minimum ($x_{\rm min}$) and the adjacent maxima ($x_{\rm max}^{\rm f/r}$) of $H(x)$, we obtain

$$\begin{aligned}\Delta H_{\rm mig}^{\rm f/r} &= H\left(x_{\rm max}^{\rm f/r}\right) - H(x_{\rm min}) \\ &= \Delta H_{\rm mig}\left[\sqrt{1-\gamma^2} \mp \gamma\left(\frac{\pi}{2}\right) + \gamma \arcsin\gamma\right], \end{aligned} \tag{6}$$

with $\gamma = (2|z_i| e E a_i)/(\pi \Delta H_{\rm mig})$. In comparison with previous treatments, our approach introduces a square-root term and provides a firm theoretical basis for the arcsin term. It is also mathematically exact (for a cosinusoidal energy hypersurface and a linear field).

The first piece of supporting evidence in favor of Eq. (6) is shown in Fig. 3. While the Mott-Gurney expression, Eq. (1), and the Fromhold-Cook expression, Eq. (4), do not describe $\Delta H_{\rm mig}^{\rm f/r}(E)$ satisfactorily, Eq. (6) describes $\Delta H_{\rm mig}^{\rm f/r}(E)$ over the entire range of field strengths considered. The differences may seem small, but it has to be remembered (i) that Eq. (6) is the argument for an exponential function [Eq. (2)]; and (ii) that the effect will be stronger for more highly charged ions. Migration of Hf^{4+} as well as of O^{2-} may be important for resistive switching of HfO_2 [53].

The second piece of supporting evidence is a prediction. Close inspection of Eq. (6) indicates that $\Delta H_{\rm mig}^{\rm f}$ goes to zero,

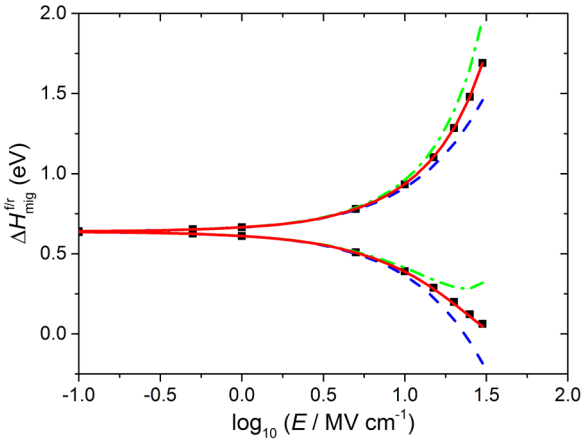

FIG. 3. Activation barriers for forward and reverse jumps, $\Delta H^{f,r}_{mig}$, as a function of field E. Symbols, NEB data; dashed line, Eq. (1); dashed dotted line, Eq. (4); solid line, Eq. (6).

as γ goes to unity (the square-root term goes to zero, and the other two terms sum to zero). On a deeper (and more simple) level this is just a consequence of the fact that, for large values of $|z_i|eE$, the maximum slope of the cosine term is smaller than $|z_i|eE$: The superimposed field is so strong, that the minima of $H(x)$ vanish. Equation (6) predicts, therefore, that there is a critical field strength E_{cr} at which the crystal is no longer stable, because the oxygen ions are no longer confined to a specific site. For oxygen ions in CeO_2, $E_{cr} = (\pi \Delta H_{mig})/(2|z_i|ea_i) \approx 36$ MV cm^{-1}. Satisfyingly, this critical value agrees very well with the results of the MD simulations: those performed at $E = 35$ MV cm^{-1} were stable, those performed at $E = 40$ MV cm^{-1} were unstable.

Lastly, we return to Fig. 1 and find that there is good agreement up to ca. $0.5E_{cr}$ between the MD data and the prediction arrived at by combining Eqs. (2) and (6). Given that ca. $0.5E_{cr}$ is an enormous field strength, the ability to describe mobility data up to this value will be sufficient for the majority of cases. In other words, this behavior shows that NEB calculations alone are sufficient to predict the field-enhanced mobility up to ca. $0.5E_{cr}$, if Eq. (6) is used. It remains to be seen whether $0.5E_{cr}$ is specific to oxygen-ion migration in CeO_2 or more generally applicable to ion migration in solids. The noticeable deviation observed for $E > 0.5E_{cr}$ is attributed to the activation entropy of migration increasing with increasing field strength. The potential well in which the migrating ion resides becomes increasingly anharmonic and broader with increasing field, causing ν_0 to decrease. This leaves ΔS_{mig} as the only quantity remaining, at least in the framework of Eq. (2), that can deliver the required increase in u_i. Calculations of the effect of E on ΔS_{mig} are, however, outside the scope of this letter.

In summary, we used atomistic simulation techniques to test analytical expressions that predict the behavior of the ion mobility in a crystalline oxide under an applied field. Simulations were performed up to field strengths that are difficult to apply in standard transport experiments but that are easily reached in resistive switching devices, in the oxidation of metals, and in atomic force and scanning-tunneling microscopy (AFM, STM) studies, and that may be reached in space-charge layers at interfaces and in nanoscale batteries and fuel cells. We find that the standard Mott-Gurney expression is only able to describe $u_i(E)$ in the very weak-field regime (increases in u_i of 20–30%). We use a new procedure to derive superior analytical expressions for $\Delta H^{f/r}_{mig}(E)$ and hence $u_i(E)$. Our approach predicts a critical field strength at which the crystal becomes unstable (E_{cr}). Furthermore, it describes exactly $\Delta H^{f/r}_{mig}(E)$ up to E_{cr} and $u_i(E)$ up to ca. $0.5E_{cr}$. Thus, we have not only elucidated the limits of the standard Mott-Gurney expression for u_i, we have also obtained a superior expression, and we propose a general procedure to examine field-enhanced ion migration in solids with complex energy hypersurfaces.

We acknowledge discussions with S. Genreith, I. Valov and F. Gunkel; financial support from the Fonds der Chemischen Industrie, Germany, and the German Research Foundation (DFG) within the framework of the collaborative research center "Nanoswitches" (SFB 917); and computing resources from JARA-HPC under project jara0100.

[1] E. J. W. Verwey, Physica **2**, 1059 (1935).
[2] N. F. Mott and R. W. Gurney, *Electronic Processes in Ionic Crystal*, 2nd ed. (Oxford University Press, Oxford, 1950).
[3] N. Cabrera and N. F. Mott, Rep. Prog. Phys. **12**, 163 (1949).
[4] K. R. Lawless, Rep. Prog. Phys. **37**, 231 (1974).
[5] R. Waser and M. Aono, Nat. Mater. **6**, 833 (2007).
[6] R. Waser, R. Dittmann, G. Staikov, and K. Szot, Adv. Mater. **21**, 2632 (2009).
[7] D. S. Jeong, R. Thomas, R. S. Katiyar, J. F. Scott, H. Kohlstedt, A. Petraru, and C. S. Hwang, Rep. Prog. Phys. **75**, 076502 (2012).
[8] J. J. Yang, D. B. Strokov, and D. R. Stewart, Nat. Nanotechnol. **8**, 13 (2013).
[9] I. Valov, ChemElectroChem **1**, 26 (2014).
[10] C. Baeumer, C. Schmitz, A. H. H. Ramadan, H. Du, K. Skaja, V. Feyer, P. Müller, B. Arndt, C.-L. Jia, J. Mayer, R. A. De Souza, C. M. Schneider, R. Waser, and R. Dittmann, Nat. Commun. **6**, 8610 (2015).
[11] S. Menzel, M. Waters, A. Marchewka, U. Böttger, R. Dittmann, and R. Waser, Adv. Funct. Mater. **21**, 4487 (2011).
[12] D. B. Strukov and R. S. Williams, Appl. Phys. A **94**, 515 (2009).
[13] D. Ielmini, IEEE Trans. Electron Devices **58**, 4309 (2011).
[14] M. Noman, W. Jiang, P. A. Salvador, M. Skowronski, and J. A. Bain, Appl. Phys. A **102**, 877 (2011).
[15] S. Larentis, F. Nardi, S. Balatti, D. C. Gilmer, and D. Ielmini, IEEE Trans. Electron Devices **59**, 2468 (2012).
[16] B. Roling, S. Murugavel, A. Heuer, L. Luhning, R. Friedrich, and S. Rothel, Phys. Chem. Chem. Phys. **10**, 4211 (2008).
[17] I. Valov and W. D. Lu, Nanoscale **8**, 13828 (2016).
[18] A. Vahed and D. A. R. Kay, Metall. Trans. B **7**, 375 (1976).
[19] D. Y. Wang and A. Nowick, J. Solid State Chem. **35**, 325 (1980).
[20] X. Guo, W. Sigle, and J. Maier, J. Am. Ceram. Soc. **86**, 77 (2003).
[21] X. Guo and R. Waser, Prog. Mater. Sci. **51**, 151 (2006).
[22] A. Tschoepe, S. Kilassonia, and R. Birringer, Solid State Ionics **173**, 57 (2004).

[23] H. J. Avila-Paredes, K. Choi, C.-T. Chen, and S. Kim, J. Mater. Chem. **19**, 4837 (2009).
[24] H. B. Lee, F. B. Prinz, and W. Cai, Acta Mater. **61**, 3872 (2013).
[25] D. S. Mebane and R. A. De Souza, Energy Environ. Sci. **8**, 2935 (2015).
[26] R. Meyer, X. Guo, and R. Waser, Electrochem. Solid-State Lett. **8**, E67 (2005).
[27] M. Gellert, K. I. Gries, C. Yada, F. Rosciano, K. Volz, and B. Roling, J. Phys. Chem. C **116**, 22675 (2012).
[28] S. Murugavel and B. Roling, J. Non-Cryst. Solids **351**, 2819 (2005).
[29] A. Heuer, S. Murugavel, and B. Roling, Phys. Rev. B **72**, 174304 (2005).
[30] M. Kunow and A. Heuer, J. Chem. Phys. **124**, 214703 (2006).
[31] D. A. Andersson, S. I. Simak, N. V. Skorodumova, I. A. Abrikosov, and B. Johansson, Proc. Natl. Acad. Sci. USA **103**, 3518 (2006).
[32] M. Nakayama and M. Martin, Phys. Chem. Chem. Phys. **11**, 3241 (2009).
[33] B. Grope, T. Zacherle, M. Nakayama, and M. Martin, Solid State Ionics **225**, 476 (2012).
[34] S. Grieshammer, B. O. H. Grope, J. Koettgen, and M. Martin, Phys. Chem. Chem. Phys. **16**, 9974 (2014).
[35] P. P. Dholabhai, J. B. Adams, P. Crozier, and R. Sharma, J. Chem. Phys. **132**, 094104 (2010).
[36] R. A. De Souza, A. Ramadan, and S. Horner, Energy Environ. Sci. **5**, 5445 (2012).
[37] A. R. Genreith-Schriever, P. Hebbeker, J. Hinterberg, T. Zacherle, and R. A. De Souza, J. Phys. Chem. C **119**, 28269 (2015).
[38] J. Faber, C. Geoffroy, A. Roux, A. Sylvestre, and P. Abélard, Appl. Phys. A **49**, 225 (1989).
[39] K. Fuda, K. Kishio, S. Yamauchi, and K. Fueki, J. Phys. Chem. Solids **46**, 1141 (1985).
[40] S. B. Adler, J. W. Smith, and J. A. Reimer, J. Chem. Phys. **98**, 7613 (1993).
[41] B. Steele, Solid State Ionics **129**, 95 (2000).
[42] H. Inaba and H. Tagawa, Solid State Ionics **83**, 1 (1996).
[43] M. Mogensen, N. M. Sammes, and G. A. Tompsett, Solid State Ionics **129**, 63 (2000).
[44] M. Born and J. E. Mayer, Z. Phys. **75**, 1 (1932).
[45] See Supplemental Material at http://link.aps.org/supplemental/10.1103/PhysRevB.94.224304 for details regarding MD and NEB simulations. Also included is a video of an unstable simulation cell at high fields.
[46] G. Balducci, J. Kapar, P. Fornasiero, M. Graziani, M. S. Islam, and J. D. Gale, J. Phys. Chem. B **101**, 1750 (1997).
[47] T. X. T. Sayle, S. C. Parker, and D. C. Sayle, Phys. Chem. Chem. Phys. **7**, 2936 (2005).
[48] T. X. T. Sayle, S. C. Parker, and D. C. Sayle, J. Mater. Chem. **16**, 1067 (2006).
[49] T. X. T. Sayle, S. C. Parker, and D. C. Sayle, Faraday Discuss. **134**, 377 (2007).
[50] S. Plimpton, J. Comput. Phys. **117**, 1 (1995).
[51] A. T. Fromhold and E. L. Cook, J. Appl. Phys. **38**, 1546 (1967).
[52] G. Henkelman, B. P. Uberuaga, and H. Jónsson, J. Chem. Phys. **113**, 9901 (2000).
[53] A. Wedig, M. Luebben, D.-Y. Cho, M. Moors, K. Skaja, V. Rana, T. Hasegawa, K. K. Adepalli, B. Yildiz, R. Waser, and I. Valov, Nat. Nanotechnol. **11**, 67 (2016).